Reprinted from JOURNAL OF THE ELECTROCHEMICAL SOCIETY
Vol. 142, No. 8, August 1995
Printed in U.S.A.

Modeling of Proton Exchange Membrane Fuel Cell Performance with an Empirical Equation

Junbom Kim,*,[a] Seong-Min Lee,,[b] and Supramaniam Srinivasan****

Center for Electrochemical Systems and Hydrogen Research, Texas Engineering Experiment Station, Texas A&M University System, College Station, Texas 77843-3402, USA

Charles E. Chamberlin

Department of Environmental Resources Engineering, Humboldt State University, Arcata, California 95521, USA

ABSTRACT

An empirical equation [$E = E_0 - b \log i - Ri - m \exp(ni)$] was shown to fit the experimental cell potential (E) *vs.* current density (i) data for proton exchange membrane fuel cells (PEMFCs), at several temperatures, pressures, and oxygen compositions in the cathode gas mixture. The exponential term compensates for the mass-transport regions of the E *vs.* i plot; *i.e.*, the increase in slope of the pseudolinear region and the subsequent rapid fall-off of the cell potential with increasing current density. As has been previously shown, the terms E_0 and b yield the electrode kinetic parameters for oxygen reduction in the PEMFC and R represents the resistance, predominantly ohmic and, to a small extent, the charge-transfer resistance of the electro-oxidation of hydrogen. The exponential term characterizes the mass-transport region of the E *vs.* i plot. The parameter n has more pronounced effects than the parameter m in this region. A physicochemical interpretation of these parameters is needed.

Introduction

Interest in the development of low or zero emission vehicles (ZEVs) is gaining momentum due to the ever-increasing environmental problems caused by the internal combustion engine and diesel engine powered vehicles, particularly in cities with high densities of population. The only known types of power sources for ZEVs are batteries, fuel cells (H_2 fed), and their hybrids. The proton exchange membrane fuel cell (PEMFC) is the most promising candidate fuel cell power source for a ZEV, because of its desirable characteristics, such as quick start capability, low operating temperature, high energy efficiency, and high power density.

Air is the logical oxidant for PEMFCs, but mass-transport overpotential in the medium to high current density region is a major problem. Since the early 1960s, several modeling studies have been carried out to elucidate the cell and half-cell potential (E) *vs.* current density (i) behavior, and also the current distribution in porous electrodes.[1-4] Reference 1 presents a comprehensive review of the papers published in the 1960s, while Ref. 2 to 4 present original contributions and briefly review the relevant literature after the 1960s. Analytic expressions for the E *vs.* i behavior and for the current distribution have been developed in special cases, for instance when the electrode reactions are either activation and ohmic or activation and mass-transport controlled. However, when all forms of overpotential (activation, mass-transport, and ohmic) are present, as at higher current densities, particularly when air is used as the cathodic reactant, there are no analytic solutions for the second order differential equations; thus interpretations of the E *vs.* i plots and of the current distribution have been made using numerical methods.

In this paper we demonstrate the excellent fit of the E *vs.* i data to an empirical equation. For this purpose, the experimental results of two investigations in our laboratory (Center for Electrochemical Systems and Hydrogen Research, CESHR) were used, one was on a PEMFC with porous gas-diffusion electrodes, fabricated in-house, and Nafion® 115 membrane and the other on a PEMFC with E-TEK electrodes and Asahi Chemical Aciplex®-S 1004 membrane.[4] The importance of this equation is that it could be used to (i) model the performance of fuel-cell power plants with respect to power density, energy efficiency, and waste heat generation rates as functions of current density; and (ii) suggest approaches for optimization of structures of the electrodes, membrane and electrode assemblies, and of the operating conditions. The analysis of the results in this paper demonstrated that there is a significant decrease in the value of the parameter n with decrease of mass-transport overpotential. Thus, to minimize mass-transport overpotential, one must optimize the structure of the electrode, increase the O_2 concentration, and/or increase the temperature to reduce the value of n.

Experimental

The experimental studies focused on the performance evaluation of proton exchange membrane fuel cells (electrode area 50 cm^{-2}) with low platinum loading electrodes (0.4 Pt mg cm^{-2}) and Nafion® 115 membranes. The electrodes were prepared by the rolling method.[5] Briefly described, this procedure consisted of using a heavy stainless steel roller (40 cm^2 long and 20 cm in diam) to prepare the diffusion and electrocatalyst layers which were subsequently rolled onto the carbon cloth substrate. The Teflon content of the carbon cloth substrate, diffusion layer, and electrocatalyst layer was 40, 35, and 30%, respectively. The electrodes were impregnated with Du Pont Nafion solution, as described previously; the Nafion content of the electrode was 0.6 mg cm^{-2}. The Nafion 115 membrane was cleaned with 5% H_2O_2 and 1N H_2SO_4 at 80°C each for about an hour.[4] In between and after the above cleaning treatments, the Nafion 115 membrane was repeatedly kept in water a few times for an hour each time at this temperature. The membrane and electrode assembly was prepared by hot-pressing the Nafion impregnated electrodes to the Nafion membrane at 130°C (a temperature slightly above the glass transition temperature of the membrane). Thereafter, the membrane and electrode assembly was incorporated in the single-cell test fixture, and the single-cell test fixture connected to the fuel-cell test station. The PEMFC was conditioned by operation with H_2/O_2 as reactants at 50°C and 1 atm at a current density of 100 mA cm^{-2} for ~24 h. The cell potential *vs.* current density measurements were then recorded using the computer, interfaced with the fuel-cell test station. The fuel was always pure H_2 (99.99% purity), and the oxidant was oxygen of the same purity or house air, the latter precleaned to remove organic contaminants. The flow rates were 1.2 times stoichiometric on the fuel side and 2 times stoichiometric on the oxidant side.

* Electrochemical Society Student Member.
** Electrochemical Society Active Member.
[a] Present address: Department of Chemical Engineering, Ulsan University, Ulsan, Kyoungnam 680-749, Korea.
[b] Present address: Korea Gas Corporation, Research and Development Center, Ansan, Kyunggi 425-150, Korea.

Table I. Calculated values of electrode kinetic parameters from a typical set of PEMFC performance data by a nonlinear regression analysis using Eq. 1 and 5.

Item	Units	Equation 1		Equation 5	
		Value of parameter	Standard deviation	Value of parameter	Standard deviation
Parameters					
E_o	mV	981	2	982	2
b	mV dec^{-1}	66.9	1.5	68.9	1.2
R	$\Omega \cdot cm^2$	0.355	0.010	0.328	0.007
m	mV	—	—	0.125	0.025
n	cm^2 mA^{-1}	—	—	0.00945	0.00023
Sample size	—	72	—	139	—
Standard deviation	mV	2.3	—	3.1	—
Correlation coefficient	—	0.9982	—	0.9997	—

Development of Model

The relationship between cell potential and current density in the low and intermediate current density region (*i.e.*, activation and ohmic controlled) of a PEMFC has been shown[5] to obey the equation

$$E = E_0 - b \log i - Ri \quad [1]$$

where

$$E_0 = E_r + b \log i_0 \quad [2]$$

E_r is the reversible potential for the cell, i_o and b are the Tafel parameters for oxygen reduction, and R represents the resistance which causes a linear variation of E with i. The predominant contribution to R is the ohmic resistance of the proton exchange membrane; the other contributions to R are the charge-transfer resistance of the hydrogen oxidation reaction, the electronic resistance of the single-cell test fixtures, and mass-transport resistance in the intermediate current density region.

A nonlinear parameter estimation software was used to determine the parameters (E_o, b, and R) in Eq. 1. Such calculations generally yield precise values of these parameters with correlation coefficients in excess of 0.99, as shown in Table I. At higher current densities, the cell potential decreases much more rapidly than expected according to Eq. 1 (Fig. 1). The difference (ΔE) between the observed cell potential and that predicted by Eq. 1 at any value of current density in this region provides an estimate of the overpotential due to mass-transport limitations.

Several modeling studies[2-4] have been conducted to interpret the cell potential *vs.* current density behavior over the entire current density region. Attempts have been made to rationalize the mass-transport regions in the E *vs.* i plots which are illustrated by (*i*) an increase in slope of the linear region with decreasing partial pressure of oxygen and (*ii*) the departure of these plots from linearity. The generally accepted interpretations are that mass-transport limitations are caused either by a change in porosity and/or tortuosity in the diffusion layer of the electrode or by the presence of water droplets or films in the diffusion layer. However, as stated in the Introduction, in none of the previous modeling studies was it possible to obtain an analytic expression for the cell potential *vs.* current density plot over the entire current density region. Numerical analyses were necessary to solve the differential equations with the appropriate boundary conditions.

An ingenious method[6] was adopted by one of the authors of this paper (C.E.C.) to find an expression to account for the departure from linearity of the cell potential *vs.* current density plot. Chamberlin showed that a plot of ΔE (the difference between the expected value of E based on Eq. 1 and the experimental value) *vs.* log i is linear, as in Fig. 2. Thus ΔE may be expressed as an exponential function of the current density, *i.e.*

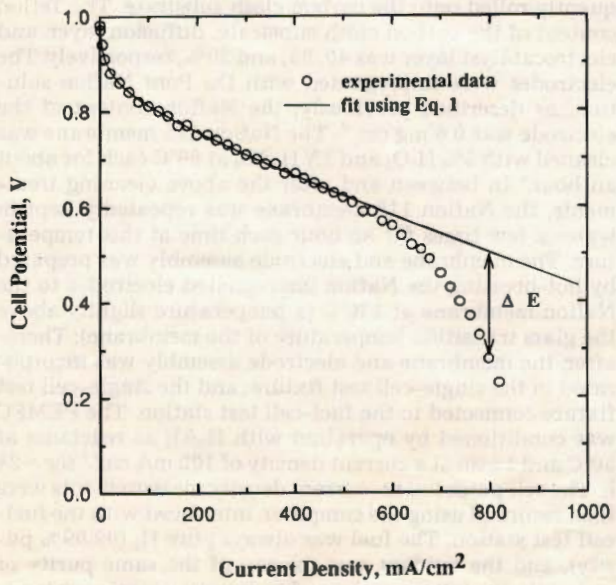

Fig. 1. Modeling of E *vs.* i curves using Eq. 1, $E = E_o - b \log i - Ri$.

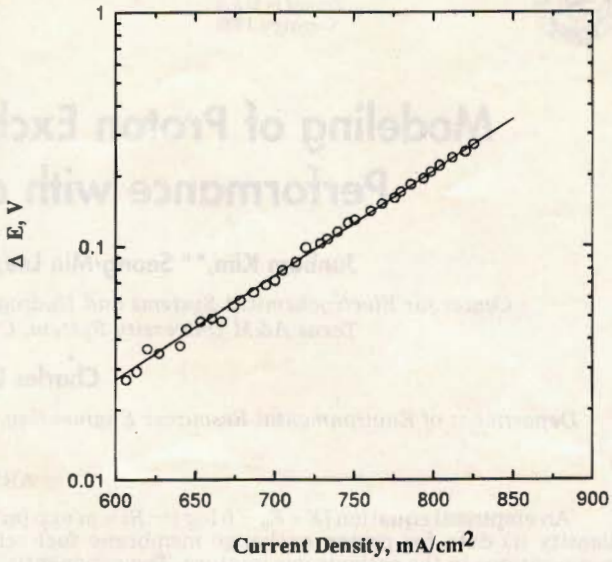

Fig. 2. Overpotential due to mass-transport limitation as a function of current density.

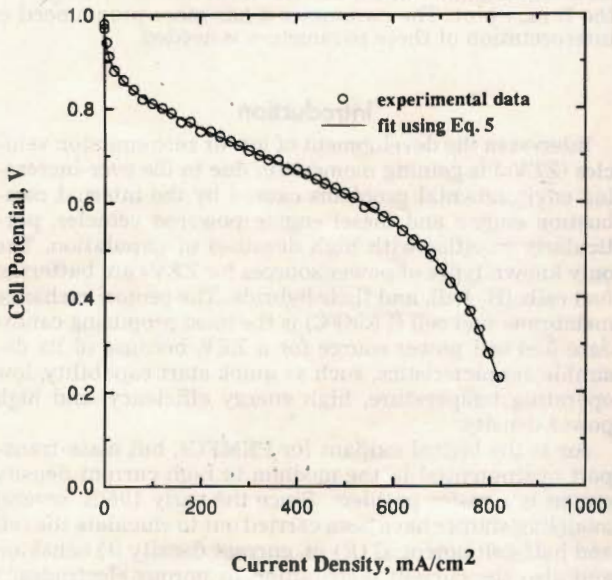

Fig. 3. Modeling of E *vs.* i curve using Eq. 5, $E = E_o - b \log i - Ri - m \exp(ni)$.

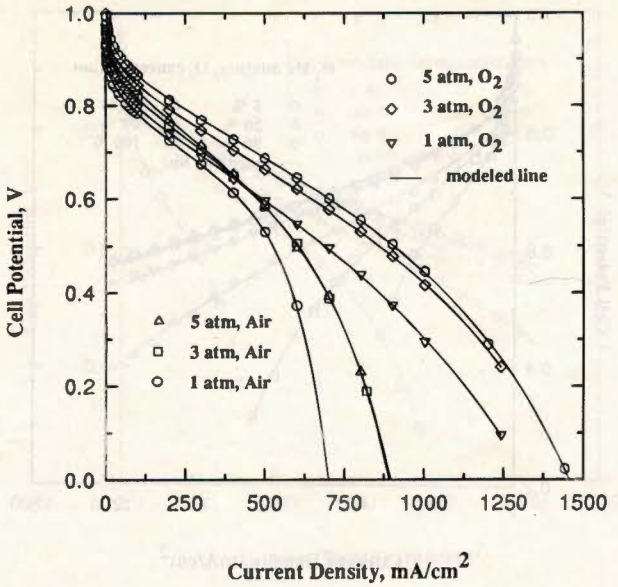

Fig. 4. Cell potential *vs.* current density plot in a PEMFC with CESHR electrodes and Nafion 115 membrane at 50°C. Solid lines are based on Eq. 5.

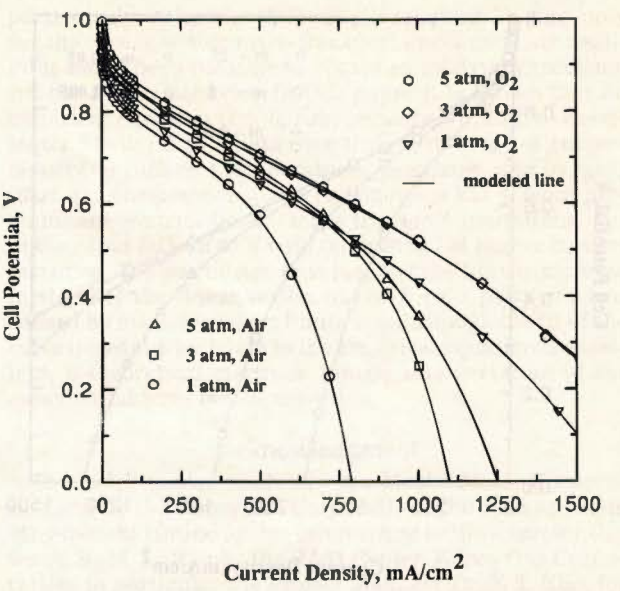

Fig. 5. Cell potential *vs.* current density plot in a PEMFC with CESHR electrodes and Nafion 115 membrane at 70°C. Solid lines are based on Eq. 5.

$$\Delta E = m \exp(ni) \quad [3]$$

where m and n are constants and have the units of potential and reciprocal of current density, respectively. The parameters m and n, which account for the mass-transport overpotential as a function of current density, can then be obtained by a nonlinear regression analysis. Another equation

$$\Delta E = mi^n \quad [4]$$

was shown by Chamberlin to account for the departure from linearity of the E *vs.* i plot, but Eq. 3 was shown to have a better fit. A combination of Eq. 1 and 3 gives

$$E = E_0 - b \log i - Ri - m \exp(ni) \quad [5]$$

This equation describes the E *vs.* i plot over the entire current density range, as illustrated in Fig. 3. Table I also shows that the values of E_0, b, and R, calculated using Eq. 5, are statistically as significant, or even more so, than calculated by using Eq. 1, which is valid for the experimental data only up to a current density of 400 mA cm^{-2}.

To understand better the electrode kinetic and mass-transport parameters, as derived from the empirical equation, we must draw correlations between the parameters in Eq. 1 and 5. This can be done by linearization of the exponential term in Eq. 5 for low values of i. Thus, Eq. 5 reduces to

$$E \cong (E_0 - m) - b \log i - (R + mn)i \quad [6]$$

When the coefficients of the terms in Eq. 1 and 6 are compared, there are three correlations

$$E_{0,1} = E_{0,5} - m \quad [7]$$

$$b_1 = b_5 \quad [8]$$

$$R_1 = R_5 + mn \quad [9]$$

The subscripts 1 and 5 denote that the parameters originate from Eq. 1 and 5, respectively. Since the values of m and n are positive, the fitting using Eq. 5 results in higher values for E_0 and lower values for R than when using Eq. 1; the Tafel slope remains the same in both cases.

Demonstration of Excellent Fit of Empirical Equation

PEMFC with CESHR electrodes and Nafion 115 proton conducting membrane.—Chamberlin demonstrated[6] that Eq. 5 fits the data of cell potential *vs.* current density, for PEMFCs set up and operated at Humboldt State University (HSU). A more detailed testing of this empirical equation is made here using the experimental performance data obtained in PEMFCs at Texas A&M University (TAMU). Ex-

Table II. Electrode kinetic and mass-transport parameters for a PEMFC with CESHR electrodes (0.3 mg Pt/cm^2) and Nafion 115 membrane calculated using Eq. 1 and 5.

Reactant	Temperature (°C)	Pressure (atm)	E_o (mV) Eq. 1	E_o (mV) Eq. 5	b (mV/dec) Eq. 1	b (mV/dec) Eq. 5	R ($\Omega \cdot$ cm^2) Eq. 1	R ($\Omega \cdot$ cm^2) Eq. 5	m (mV) Eq. 5	n (cm^2/mA) Eq. 5
H_2/Air	50	1	942	943	61	62	0.390	0.363	3.80×10^{-1}	1.03×10^{-2}
		3	973	978	57	60	0.434	0.363	2.90	5.72×10^{-3}
		5	987	991	55	57	0.472	0.406	3.08	5.59×10^{-3}
	70	1	937	943	58	62	0.344	0.238	3.75	6.38×10^{-3}
		3	981	982	58	59	0.321	0.306	3.60×10^{1}	6.53×10^{-3}
		5	994	1000	55	57	0.338	0.280	5.20	3.61×10^{-3}
H_2/O_2	50	1	957	979	60	62	0.391	0.300	2.15×10^{1}	2.17×10^{-3}
		3	1005	1010	63	64	0.348	0.313	3.40	3.21×10^{-3}
		5	1022	1027	61	63	0.345	0.298	4.63	3.05×10^{-3}
	70	1	956	970	58	60	0.317	0.259	1.25×10^{1}	2.10×10^{-3}
		3	1012	1024	61	63	0.278	0.231	1.01×10^{1}	2.00×10^{-3}
		5	1004	1032	52	54	0.313	0.242	2.57×10^{1}	1.45×10^{-3}

Eq. 1: $E = E_o - b \log i - Ri$, valid up to the end of linear region of E *vs.* i plot.
Eq. 5: $E = E_o - b \log i - Ri - m \exp(ni)$, valid over the entire range of E *vs.* i plot.

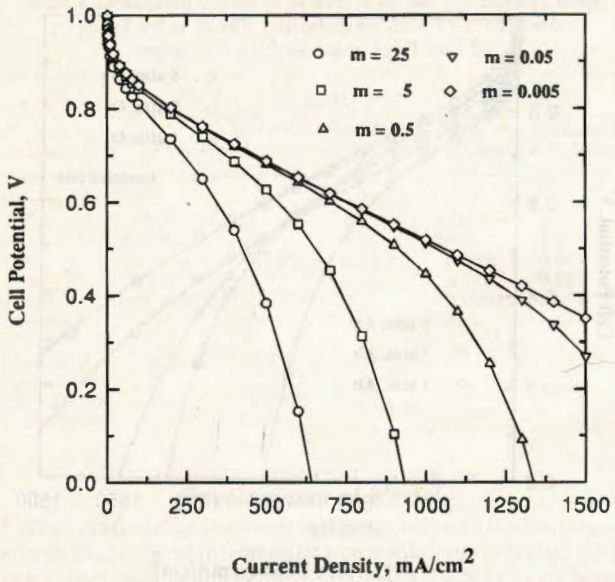

Fig. 6. Dependence of cell potential *vs.* current density plot on value of m (mV) in Eq. 5, assuming that E_o = 1000 mV, b = 60 mV/dec, R = 0.3 Ω · cm², and $n = 5 \times 10^{-3}$ cm² mA⁻¹.

periments were conducted on a PEMFC, with a Nafion 115 proton conducting membrane and electrodes containing 0.3 mg Pt/cm² (prepared at TAMU) at two temperatures and three pressures. In Fig. 4 and 5, the symbols represent the experimental data of the cell potential *vs.* current density at 50 and 70°C, respectively, and the solid line represents the fit of the experimental data to Eq. 5. The excellent fit of the experimental data to the empirical equation is demonstrated. The calculated values of the electrode kinetic and mass-transport parameters using Eq. 1 and 5 are shown in Table II. As expected from Eq. 7 and 9, the E_0 value is higher, and the R value is smaller, when using Eq. 5 rather than Eq. 1. The b values, found using Eq. 1 and 5, are comparable.

The parameters m and n describe mass-transport limitations; thus one expects a dependence of m and/or n on physicochemical parameters such as temperature and pressure. This dependence is not apparent from the results in Table II. Since an interpretation of the m and n values is essential for an understanding of mass-transport limitations, the effect of variation of m and of n on the cell potential *vs.* current density behavior was theoretically evaluated. For this purpose, the parameters E_o, b, and R were arbitrarily set at constant but experimentally obtainable values, and only the m or n value was changed. The m value affects both the slope of the linear region of the E *vs.* i plot and the current density at which there is departure of this plot from linearity (Fig. 6). The n value has a major effect on the dependence of E *vs.* i after the linear region, *i.e.*, the rapid fall-off of E with increasing i, the major mass-transport limitation region (Fig. 7). The value of n has only a small effect on the slope of the linear region; its dominant effect is in dramatically changing the slope of the E *vs.* i plot in the major mass-transport limitation region. As a consequence, it determines the apparent limiting current density. A more detailed analysis of the parameters m and n is provided in the following section.

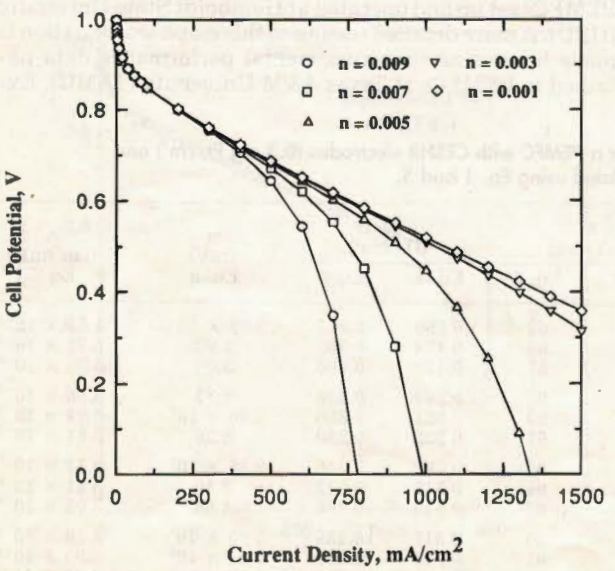

Fig. 7. Dependence of cell potential *vs.* current density plot on value of n (cm² mA⁻¹) in Eq. 5, assuming that E_o = 1000 mV, b = 60 mV/dec, R = 0.3 Ω · cm², and m = 0.5 mV.

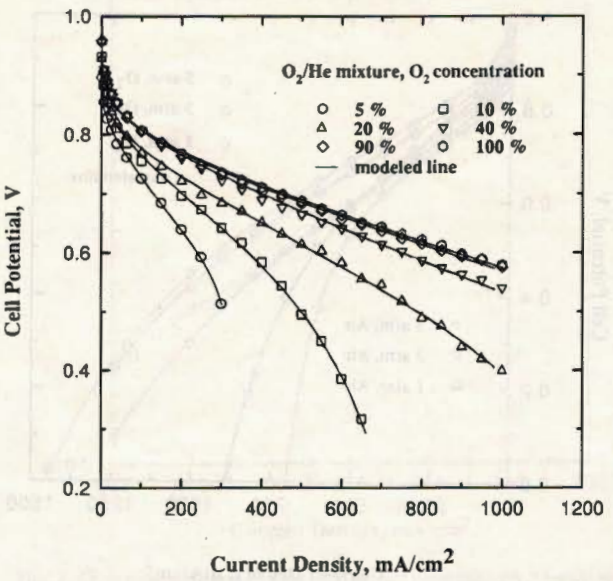

Fig. 8. Effect of He concentration on cell potential *vs.* current density plot in a PEMFC with E-TEK electrode and Asahi Chemical Aciplex-S membrane at 1 atm, 60°C, and a 1.5 stoichiometric flow rate.[4] Solid lines are based on Eq. 5.

PEMFC with E-TEK electrode and Aciplex-S 1004 proton conducting membrane fed with O_2/He, O_2/Ar, and O_2/N_2

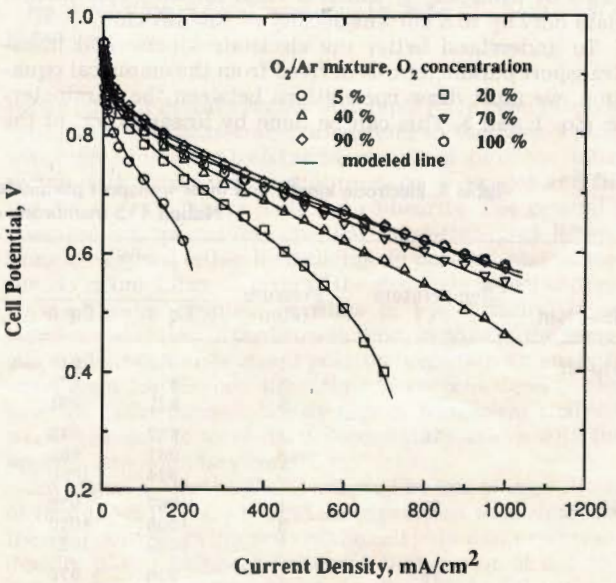

Fig. 9. Effect of Ar concentration on cell potential *vs.* current density plot in a PEMFC with E-TEK electrode and Asahi Chemical Aciplex-S membrane at 1 atm, 60°C, and a 1.5 stoichiometric flow rate.[4] Solid lines are based on Eq. 5.

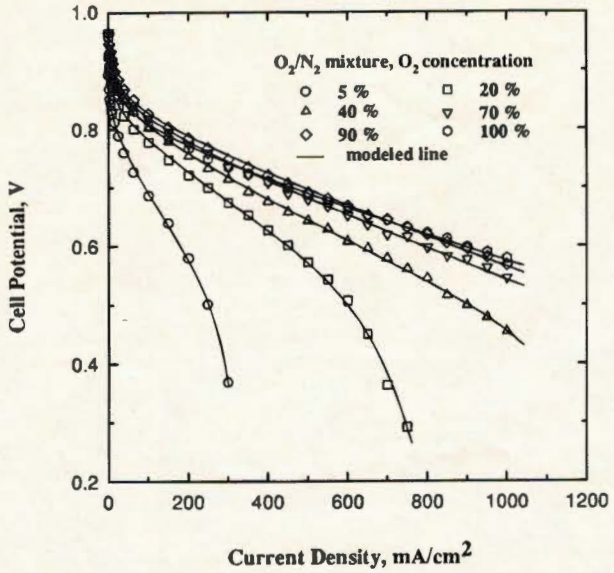

Fig. 10. Effect of N_2 concentration on cell potential *vs.* current density plot in a PEMFC with E-TEK electrode and Asahi Chemical Aciplex-S membrane at 1 atm, 60°C, and a 1.5 stoichiometric flow rate.[4] Solid lines are based on Eq. 5.

mixtures.—A systematic analysis was made using previously published performance data[4] of a PEMFC with E-TEK electrodes, Aciplex-S 1004 proton conducting membrane from Asahi Chemical Co. Ltd., and O_2/inert gas mixtures as cathodic reactants. Figures 8-10 demonstrate the effects of the composition of oxygen in the gas mixtures of O_2/He, O_2/Ar, or O_2/N_2, respectively, on the dependence of E on i plots. The calculated values of the electrode kinetic and mass-transport parameters, using Eq. 5, are listed in Table III. The solid lines in Fig. 8-10 represent the excellent fit of the experimental data to this equation. From Table III, it is seen that the value m covers a wide range, 10^{-19} to 10^{0}, whereas the value of n is in a relatively narrow range. When mass transport limitations are minimal, the m values are in the range 10^{-19} to 10^{-9}. Higher values of m clearly demonstrate mass-transport limitations. The relatively high values of the parameter n, however, are indicative of significant mass-transport overpotentials.

Conclusion

Several modeling studies have been carried out previously to analyze the behavior of performance in PEMFCs particularly with air as the cathodic reactant. To date, only for the case in which mass-transport limitations are negligible has it been possible to obtain an analytic expression for the E *vs.* i behavior. In this paper it is shown that an empirical equation (Eq. 5, first published in Ref. 6) excellently fits the E *vs.* i data over the entire range of current density, at different temperatures, pressures, and oxygen/inert gas compositions. The parameter n has a more predominant contribution to mass-transport limitations, *i.e.*, in the rapid fall-off of E with increasing i at higher current densities. The parameter m is responsible for the increase in slope of the linear region of the E *vs.* i plot, which is caused by mass-transport limitations. Though the fit of the experimental E *vs.* i data to the empirical equation is excellent, a theoretical electrode kinetic interpretation of the exponential term is still needed.

Acknowledgment

This work was sponsored by the Mazda Motor Corporation and by the Korea Gas Corporation. The authors thank Mr. Shinichi Hirano for his interest and enthusiasm for this work. S.-M. L. thanks the R&D Center, Korea Gas Corporation, in particular the Project Manager Dr. Y. T. Kho, for providing the opportunity to perform this investigation at CESHR.

Manuscript submitted Nov. 7, 1994; revised manuscript received Feb. 2, 1995. This was in part Paper 12 presented at the San Francisco, CA, Meeting of the Society, May 22-27, 1994.

The Center for Electrochemical Systems and Hydrogen Research assisted in meeting the publication costs of this article.

REFERENCES

1. J. O'M. Bockris and S. Srinivasan, *Fuel Cells: Their Electrochemistry,* McGraw-Hill Book Company, New York (1969). Chapter 5 contains a review of the work in the 1960s.
2. T. E. Springer and S. Gottesfeld, *This Journal,* **140,** 3513 (1993).
3. D. M. Bernardi and M. W. Verbrugge, *ibid.,* **139,** 2477 (1992).
4. Y. W. Rho, O. A. Velev, S. Srinivasan, and Y. T. Kho, *ibid.,* **141,** 2089 (1994).
5. S. Srinivasan, E. A. Ticianelli, C. R. Derouin, and A. Redondo, *J. Power Sources,* **22,** 359 (1988).
6. C. E. Chamberlin, P. A. Lehman, R. M. Reid, and T. G. Herron, in *Hydrogen Energy Progress X,* D. Block and T. N. Veziroglu, Editors, Proceedings of the 10th World Hydrogen Energy Conference, Cocoa Beach, FL, June 20-24, 1994, Vol. 3, pp. 1659-1668, International Association for Hydrogen Energy, FL (1994).

Table III. Electrode kinetic and mass-transport parameters, for a PEMFC with E-TEK electrodes (0.4 mg Pt/cm^2) and Aciplex-S 1004 membrane using O_2/inert gas mixture as the cathodic reactant at 1 atm and 60°C, calculated using Eq. 5

Reactant gas mixture	O_2 (%)	E_o (mV)	b (mV/dec)	R ($\Omega \cdot$ cm^2)	m (mV)	n (cm mA^{-1})
O_2/He	5	881	38	0.776	6.39×10^{-4}	3.69×10^{-2}
	10	916	52	0.451	1.08	7.73×10^{-3}
	20	915	53	0.307	2.61×10^{-1}	5.34×10^{-3}
	40	947	58	0.239	1.68×10^{-10}	2.91×10^{-3}
	90	946	60	0.198	1.28×10^{-19}	1.69×10^{-2}
	100	945	58	0.196	1.98×10^{-10}	3.28×10^{-3}
O_2/Ar	5	890	46	0.751	1.33×10^{-4}	5.78×10^{-2}
	20	930	48	0.430	2.76×10^{-2}	1.17×10^{-2}
	40	937	48	0.311	4.05×10^{-3}	8.47×10^{-3}
	70	948	50	0.254	1.40×10^{-10}	2.69×10^{-3}
	90	953	52	0.229	1.06×10^{-19}	3.36×10^{-3}
O_2/N_2	5	879	46	0.962	1.89×10^{-2}	2.89×10^{-2}
	20	917	47	0.404	1.41×10^{-1}	9.64×10^{-3}
	40	949	57	0.304	9.57×10^{-4}	9.99×10^{-3}
	70	958	57	0.246	6.79×10^{-11}	4.28×10^{-3}
	90	960	54	0.232	1.59×10^{-9}	2.16×10^{-3}

Eq. 5: $E = E_o - b \log i - Ri - m \exp(ni)$, valid over the entire range of E *vs.* i plot.